Technical Note

Study on Sound Transmission across a Floating Floor in a Residential Building by Using SEA

Xianfeng HUANG[(1), (2)*], Yimin LU[(3)], Chen QU[(1)], Chenhui ZHU[(1)]

[(1)] *College of Civil Engineering and Architecture*
Guangxi University
Nanning 530004, China
*Corresponding Author e-mail: x.f.huang@gxu.edu.cn

[(2)] *Guangxi Key Laboratory of Disaster Prevention and Engineering Safety*
Guangxi University
Nanning 530004, China

[(3)] *School of Electrical Engineering*
Guangxi University
Nanning 530004, China

For the purpose of reducing the impact noise transmission across floating floors in residential buildings, two main sound transmission paths in the floating floor structure are considered: the stud path and the cavity path. The sound transmission of each path is analysed separately: the sound transmission through the cavity and the stud are predicted by statistical energy analysis (SEA). Then, the sound insulation prediction model of the floating floor is established. There is reasonable agreement between the theoretical prediction and measurement, and the results show that a resilient layer with low stiffness can attenuate the sound bridge effect, resulting in higher impact noise insulation. Then, the influences of the floor covering, the resilient layer and the floor plate on the impact sound insulation are investigated to achieve the optimised structure of the floating floor based on the sound insulation.

Keywords: sound transmission; floating floor; impact noise; sound insulation.

1. Introduction

Recently, the noise transmitted between residential floors has become an important social problem. Impact noise acting on the floor is an annoying sound that occurs in residential buildings, it is irritating for the occupants and results in many complaints. Many countries have issued codes and regulations to resolve the increasingly common noise disputes between rooms separated by a floor (PARK, 2015; LEE, 2009). In a dwelling building, the isolation of the impact noise on the floor is not only a weakness of the building but also one of the main problems for both architects and occupants. Sound transmission across the floor can be divided into two categories: airborne and structure-borne ones, depending on the source of noise (VIGRAN, 2008). Therefore, the building sound insulation includes airborne and structure-borne sound insulation. Airborne sound is transmitted through floors or walls separating household units, and the noise can be reduced by means of airborne sound insulation. Impact noise acting on the floor belongs to structure-borne sound generating from the building structure being irradiated by impact force (SCHIAVI *et al.*, 2015; YEON *et al.*, 2017), which directly excites the floor of the upstairs room to cause vibration (PARK *et al.*, 2015). The attenuation of this kind of sound energy in building materials is weak, so the propagation speed is faster than that in air, and the propagation distance is very long. The airborne sound insulation of a homogenous, heavy-weighted concrete floor may be satisfactory, while its impact noise insulation may be poor. According to the requirements of the "Green Building Evaluation Standard" (in China), the airborne weighted sound insulation of a floor should not be less than 45 dB, and the weighted standardised impact sound pressure level

cannot exceed 70 dB. Generally, the airborne sound insulation of a reinforced concrete floor is prone to meet the requirements, but the weighted standardised impact pressure level in a downstairs room can reach above 80 dB, which often does not satisfy the insulation requirement (Li *et al.*, 2017).

According to a current survey of occupants, the complaint about environmental noise has been at the top of the list of unsatisfactory building environmental qualities. Among the complaints, the impact sound insulation problem of the floor is particularly prominent: nearly 80% of occupants feel disappointed in impact noise insulation; they complained that upstairs walking, children running and jumping, pushing and pulling tables and chairs, and other sounds seriously affect their lives (Luo, Hu, 2012). The attenuation of floor impact noise is to provide the favourable acoustical environment to the occupants in residential buildings, therefore study on the approach of reducing floor impact sound is significant.

Architectural treatments, such as floating floors, elastic floor coverings, and resiliently supported ceilings have been adopted to attenuate impact sound acting on the floor. Of these, the floor structure with resilient layer (floating floor) is used most often because it can effectively reduce the impact sound transmission and has a strong ability to mitigate the interference of impact noise. Schiavi *et al.* (2018) quantify the acoustic performance of floating floor structures from the point of view of the improvement of impact sound level ΔL. They believe that the impact sound insulation is a key factor to evaluate the sound environment quality of residential buildings, and emphasise the significant role of the floating floor in abating the impact noise. The so called floating floor (shown in Fig. 1) reduces the impact noise level in the downstairs room by embedding a resilient layer (elastic cushion) for vibration reduction. A floating floor is a floor structure composed of a floor covering, stud (batten), resilient layer, cavity, and floor plate (reinforced concrete plate). The resilient layer has obvious attenuation effects on the impact sound acting on the floor, which can reduce the sound pressure level radiated to the downstairs room and achieve the goal of improving the impact sound insulation of the floor.
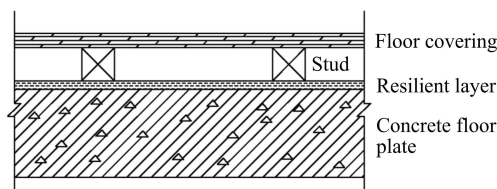

Fig. 1. Schematic diagram of the structure of a floating floor.

The common issues are concentrated on low frequency range: impact noise levels are higher in light-weighted buildings than in heavy-weighted ones. Ljunggren and Agren (2013) found that compared with heavy-weighted buildings, there is a certain risk in using a floating floor in light-weighted buildings; that is, the low-frequency sound insulation performance becomes worse due to the obvious flanking sound transmission. Although the floating floor structure can improve the impact sound insulation greatly, the low frequency sound transmission is enhanced owing to the junction coupling along the flanking sound transmission paths. In addition, the resonance matching will result in the peak impact sound pressure level at a low frequency. Based on the analysis of sound transmission in different resilient layers of floating floor structures, Cho (2013) argued that the prediction accuracy of a sound insulation model depends not only on the influence of dynamic stiffness of the resilient layer but also on the resonance matching caused by low frequency impact sound transmitted through the resilient layer in a floating floor structure. For this reason, Neves e Sousa and Gibbs (2011) established an analytical model based on experimental verification which can be used to predict low frequency impact sound transmission. The effects of impact position, floor type, boundary condition, floor and room size, receiving point position, and room absorption on low frequency impact sound transmission were studied. Hui and Ng (2007) designed a floor with a honeycomb vibration isolation device by a vibrating table test to improve the sound insulation at low frequencies (120–600 Hz).

In some specific designs of residential buildings, the installation of a resilient layer between walls and floors can also increase the sound isolation at low frequencies (Ljunggren, Agren, 2013). Thus, it can be seen that the resilient layer has a significant influence on the sound insulation of the floating floor. After further study, Kim *et al.* (2009) revealed that the stiffness of the resilient layer is a major factor affecting the sound insulation of a floor as a whole. In view of the tedious and complex theoretical prediction of sound insulation, it is common to estimate the sound insulation of a floating floor structure by engineering experience and measured data, which might lead to unacceptable errors (Kim *et al.*, 2018). Yoo and Jeon (2014) studied the effect of a resilient layer and viscoelastic damping material on reducing the impact sound across a floating floor by finite element (FE) simulation and in situ measurement. It was shown that the damping material has a higher loss factor and dynamic elastic modulus than the resilient layer. After further analysing the influence of the resilient layer on the impact sound transmission and vibration characteristics of the floor in the whole frequency range, it has been found that the impact sound transmission across a floor structure can be effectively attenuated by using damping material and resilient layer with low dynamic elastic modulus and low loss factor.

To date, the acoustic coupling mechanism of the resilient layer and the sound transmission in the viscoelastic material have not been accurately theoretically expressed, so the sound insulation mechanism of the floating floor structure with viscoelastic material layer (resilient layer) needs to be further explored. In addition, some existing studies are limited to the sound attenuation of rigid junctions, and do not include a mechanism description of the sound insulation performance of the floating floor structure, resulting in the lack of precise theoretical model to predict the isolated impact noise according to the floating floor structure of specific residential buildings. The measurements are inconsistent with the predicted results (STEWART, CRAIK, 2000). Therefore, it is necessary to predict the sound insulation of a floating floor based on the study of the sound transmission mechanism. In this paper, SEA is employed to predict the sound transmission through the cavity path and the stud path in the floor structure, and the sound insulation prediction model is established. Then, the influencing factors of impact sound insulation of the floating floor structure are analysed.

2. Theoretical description of sound transmission

In the floating floor structure shown in Fig. 1, the covering floor and the floor plate are connected by a stud and a resilient layer. The structure assembly is as follows: a resilient layer is laid on the reinforced concrete floor plate, then the wooden stud is rested on this, and the covering floor is screwed to the studs at discrete intervals by nailing. There are two main sound transmission paths across the floating floor structure: the stud path and the cavity path. According to the sound transmission characteristics of these paths, SEA theory and wave method are applied to analyse the sound transmission mechanisms on these two paths respectively.

2.1. Sound transmission through the cavity path

The sound insulation diagram of the floating floor is shown in Fig. 2. The room and floor components in Fig. 2 can be simplified as subsystems of the SEA model shown in Fig. 3. The subsystems' subscripts in
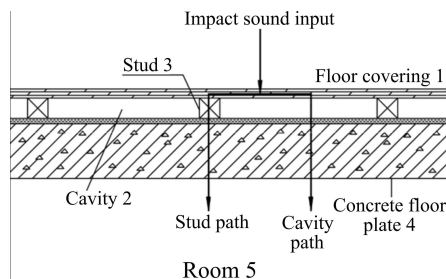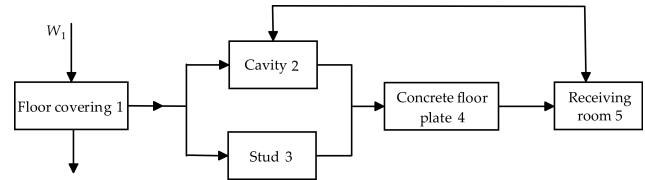

Fig. 3. SEA model of the floating floor.

the SEA model (in Fig. 3) correspond to the number of components in Fig. 2.

When a standard tapping machine is used to act on the floor (as shown in Fig. 4), bending sound waves and near field sound waves are excited. These sound waves are transmitted across the floor along the cavity path and stud path separately. The cavity path of sound transmission is along floor covering 1, cavity 2, concrete floor 4, and room 5 (as shown in Fig. 3).

Fig. 4. Tapping machine for the impact sound insulation measurements.

The resonant balance matrix equation of sound energy along the cavity path is

$$\begin{bmatrix} -\eta_1 & 0 & 0 & 0 \\ \eta_{12} & -\eta_2 & 0 & 0 \\ 0 & \eta_{24} & -\eta_4 & 0 \\ 0 & 0 & \eta_{45} & -\eta_5 \end{bmatrix} \begin{bmatrix} E_1 \\ E_2 \\ E_4 \\ E_5 \end{bmatrix} = \begin{bmatrix} -W_1/\omega \\ 0 \\ 0 \\ 0 \end{bmatrix}, \quad (1)$$

where E_i is the sound energy of each subsystem ($i = 1, 2, ..., 5$). The non-resonant balance matrix equation of sound energy along the cavity path is

$$\begin{bmatrix} -\eta_1 & 0 & 0 \\ \eta_{12} & -\eta_2 & 0 \\ 0 & \eta_{25} & -\eta_5 \end{bmatrix} \begin{bmatrix} E_1 \\ E_2 \\ E_5 \end{bmatrix} = \begin{bmatrix} -W_1/\omega \\ 0 \\ 0 \end{bmatrix}. \quad (2)$$

In Eqs (1) and (2), η_i is the total loss factor of each subsystem, η_{ij} is the coupling loss factor between subsystems, ω is the circular frequency [s^{-1}], and

Fig. 2. Schematic diagram of the floating floor.

$W_i = E_i \omega \eta_i$ is the sound power of each subsystem. According to the sound energy equilibrium matrix equation mentioned above, the sound pressure level (SPL) in room 5 (receiving room) beneath the floating floor can be obtained. The standardised impact sound pressure level along the cavity path to room 5 $L_{p,\text{air}}$ is

$$\begin{cases} L_{p,\text{air}} = 10 \times \log_{10}\left(10^{\frac{L_{p,\text{air,non}}}{10}} + 10^{\frac{L_{p,\text{air,res}}}{10}}\right), & f \le f_{c4}, \\ L_{p,\text{air}} = L_{p,\text{air,res}}, & f > f_{c4}, \end{cases}$$
$$(3)$$

where $L_{p,\text{air,non}}$ and $L_{p,\text{air,res}}$ are the non-resonant and resonant impact sound pressure level through the cavity path, f_{c4} is the critical frequency of the reinforced concrete floor plate:

$$f_{c4} = \frac{c_0^2 \sqrt{3}}{\pi h_4 c_{L4}}. \tag{4}$$

Here, c_{L4} is the longitudinal wave speed of the concrete floor plate. The non-resonant impact sound pressure level through the cavity path $L_{p,\text{air,non}}$ is

$$L_{p,\text{air,non}} = 10\log\left(\frac{p_5^2}{p_0^2}\right) = L_{w,1} + 10\log\left(\frac{\eta_{12}\eta_{25}V_1}{\eta_1\eta_2 V_5}\right)$$
$$-10\log\left(\frac{V_5}{T_5}\right) + 14. \tag{5}$$

The tapping machine is the standard excitation device for building acoustics (OLSSON, LINDERHOLT, 2019). $L_{w,1}$ which is shown as Fig. 5 is impact sound power level of the tapping machine used in measurements. The resonant impact sound pressure level through the cavity path $L_{p,\text{air,res}}$ gives

$$L_{p,\text{air,res}} = 10\log\left(\frac{p_5^2}{p_0^2}\right) = L_{w,1} + 10\log\left(\frac{\eta_{12}\eta_{24}\eta_{45}V_1}{\eta_1\eta_2\eta_4 V_5}\right)$$
$$-10\log\left(\frac{V_5}{T_5}\right) + 14, \tag{6}$$

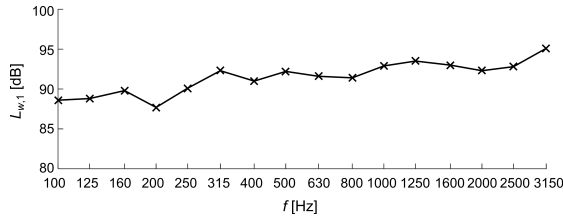where V_1 and V_5 are the volumes of floor covering 1 and room 5, respectively.

Fig. 5. L_{w1} of the tapping machine.

2.2. Sound transmission path through the stud

The stud path is along floor covering 1, stud 3, resilient layer, concrete floor plate 4, and room 5. The sound transmission coefficient τ_{14} from covering plate 1

through stud 3 and resilient layer to floor plate 4 is calculated here. In Fig. 3, the calculation model of τ_{14} which consists 4 plates and 2 junctions, it is pointed out that the number of plate is different from the number of SEA subsystem in Figs 2 and 3. The resilient layer can be modelled as a series of independent springs, and the floating floor is illustrated as shown in Fig. 6.
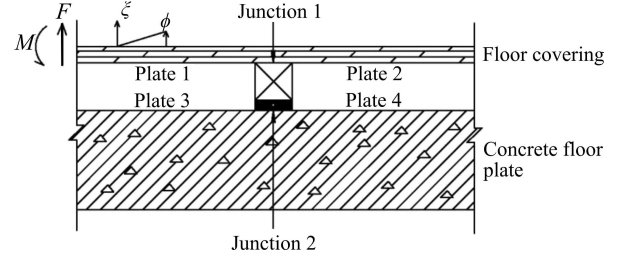
Fig. 6. Calculation model of the sound transmission coefficient τ_{14}.

When the floor covering plate is excited, bending wave and near field wave are generated. The amplitude of the bending wave is defined as T_i, the amplitude of the near field wave is T_{ni}, k_i, and k_{ni} are the bending wavenumber and near field wavenumber on plate i, where $i = 1, 2, 3, 4$. The displacements of the plates ξ can be expressed as (STEWART, CRAIK, 2000)

$$\xi_1 = (e^{-ik_1\cos\theta_1 x} + T_1 e^{ik_1\cos\theta_1 x} + T_{n1}e^{k_{n1}x})e^{-ik_1\cos\theta_1 y}e^{i\omega t},$$
$$\xi_2 = (T_2 e^{-ik_2\cos\theta_2 x} + T_{n2}e^{-k_{n2}x})e^{-ik_2\cos\theta_2 y}e^{i\omega t},$$
$$\xi_3 = (T_3 e^{ik_3\cos\theta_3 x} + T_{n3}e^{k_{n3}x})e^{-ik_3\cos\theta_3 y}e^{i\omega t}, \tag{7}$$
$$\xi_4 = (T_4 e^{-ik_4\cos\theta_4 x} + T_{n4}e^{-k_{n4}x})e^{-ik_4\cos\theta_4 y}e^{i\omega t}.$$

The displacement of the floor is caused by acoustic excitation. For each plate, the angular displacement ϕ, bending moment M, and internal force F have the following relationship with the displacement ξ:

$$\phi = \partial\xi/\partial x,$$
$$M = -B\left(\frac{\partial^2\xi}{\partial x^2} + \mu\frac{\partial^2\xi}{\partial y^2}\right), \tag{8}$$
$$F = B\left[\frac{\partial^3\xi}{\partial x^3} + (2-\mu)\frac{\partial^3\xi}{\partial x\partial y^2}\right].$$

Affected by the polar moment of inertia per unit length J and torsional stiffness of the stud per unit length T_T, the resisting moment due to rotary inertia (M_c) and torsional stiffness ($\partial M_y/\partial y$) of the stud, and the forces due to the inertia of the stud F_c and the bending forces along the direction of the stud $\partial F_y/\partial y$ are generated at the junction:

$$M_c + \frac{\partial M_y}{\partial y} = (-\omega^2 J + T_T k_2^2 \sin^2\theta_2)\phi_2,$$
$$\tag{9}$$
$$F_c + \frac{\partial F_y}{\partial y} = (-\omega^2 m' + B_c k_2^4 \sin^4\theta_2)\xi_2.$$

Then, there exists the equilibrium of displacement, angular displacement, bending moment, and internal force at junctions 1 and 2 (as shown in Fig. 6). Considering that the resilient layer has viscoelastic properties, its damping will have a certain influence on sound transmission, so it is necessary to modify its elastic modulus as a complex form $(1 + j\eta_k)E'$, where η_k is the internal loss coefficient of the resilient layer. When the floor structure is in equilibrium, then:

- equilibrium of displacement is

$$\begin{cases} \xi_1 = \xi_2, \\ \xi_3 = \xi_4, \\ \xi_1 = \xi_3 + \xi_k; \end{cases} \tag{10}$$

- equilibrium of angular displacement is

$$\begin{cases} \phi_1 = \phi_2, \\ \phi_3 = \phi_4, \\ \phi_1 = \phi_3 + \phi_k; \end{cases} \tag{11}$$

- equilibrium of internal force is

$$\begin{cases} F_1 = F_2 + F_k + F_c + \dfrac{\partial F_y}{\partial y}, \\ F_3 = F_4 - F_k; \end{cases} \tag{12}$$

- equilibrium of moment is

$$\begin{cases} M_1 = M_2 + M_k + M_c + \dfrac{\partial M_y}{\partial y}, \\ M_3 = M_4 - M_k. \end{cases} \tag{13}$$

The bending wave amplitude of each plate T_i can be obtained by the above described equilibrium equations. The sound transmission coefficient from the floor covering to the concrete floor plate τ_{14} is

$$\tau_{14} = \int\limits_0^{\pi/2} \frac{\rho_{s4}k_1\cos\theta_4}{\rho_{s1}k_4\cos\theta_1}\cos\theta\,\mathrm{d}\theta. \tag{14}$$

By neglecting the coupling of edge internal force and moment (the influence is less than 0.1 dB (STEWART, CRAIK, 2000)), the sound transmission coefficient τ_{14} can be expressed as

$$\tau_{14} = \frac{\chi\psi K^2}{2(a^*)}, \tag{15}$$

where

$$\chi = k_1/k_4, \qquad \psi = B_1 k_1^2/(B_4 k_4^2),$$

$$a^* = \chi^2\psi^2 K^2 + 2\chi\psi K^2 + K^2 - 4\chi^2\psi^2 K B_4 k_4^3$$
$$- 4KB_4\chi\psi k_4^3 + 8B_4^2\chi^2\psi^2 k_4^6.$$

At high frequencies, the thick resilient layer will result in the obvious influence of the longitudinal wave which cannot be ignored, and the elasticity stiffness K needs to be corrected according to the Gosele model (STEWART, CRAIK, 2000):

$$K = \omega\rho c_L b_3, \tag{16}$$

in which b_3 is the width of the stud [m], ρ is the density of the resilient layer [kg/m^3], and c_L is the longitudinal wave speed [m/s] in the resilient layer. The critical frequency of the resilient layer by stiffness coefficient correction is

$$f_0 = \frac{c_L}{2\pi d}, \tag{17}$$

where d is the thickness of the resilient layer, the longitudinal wave speed of the resilient layer, c_L, can be determined by elastic modulus E' and density ρ:

$$c_L = \sqrt{\frac{E'}{\rho}}. \tag{18}$$

The standardised impact sound pressure level $L_{p,\text{stud}}$ through the stud path is

$$L_{p,\text{stud}} = L_{w,1} + 10\log_{10}\left(\frac{\eta_{14}\eta_{45}V_1}{\eta_1\eta_4 V_5}\right) - 10\log_{10}\left(\frac{V_5}{T_5}\right) + 14. \tag{19}$$

2.3. Impact sound pressure level in the downstairs room (receiving chamber)

The standardised impact sound pressure level L_p in the downstairs room (receiving chamber) is

$$L_p = \begin{cases} L_{p,\text{stud}} + 10\log_{10}\left(1 + 10^{-\dfrac{L_{p,\text{stud}} - L_{p,\text{air}}}{10}}\right), \\ \qquad\qquad\qquad L_{p,\text{stud}} \geq L_{p,\text{air}}, \\ L_{p,\text{air}} + 10\log_{10}\left(1 + 10^{-\dfrac{L_{p,\text{air}} - L_{p,\text{stud}}}{10}}\right), \\ \qquad\qquad\qquad L_{p,\text{stud}} < L_{p,\text{air}}. \end{cases} \tag{20}$$

Therefore, as long as the parameters such as the total loss factor of each subsystem and the coupling loss factor between subsystems are determined, the sound transmission through the cavity path and the stud path can be calculated according to the Eqs (3), (19), and (20), respectively, and the sound pressure level coming from the corresponding path in the downstairs room can be determined.

3. Determination of parameters

3.1. Total loss factor

For the 5 subsystems of the SEA model of adjacent rooms separated by a floor, the total loss factors of these subsystems can be divided into two categories: the total loss factor of the room 5 and that of the plate. The total loss factor of the room 5 is related to the frequency and reverberation time of the room (CRAIK, SMITH, 2000):

$$\eta_i = \frac{2.2}{fT_i}, \tag{21}$$

where T_i is the room reverberation time [s]. The total loss factor of the plate is related to the thickness, longitudinal wave speed, sound absorption coefficient, and the boundary condition of the plate, which can be expressed as (CRAIK, SMITH, 2000):

$$\eta_i = 0.1365 \left(\frac{h_i c_{Li}}{f} \right)^{1/2} \frac{\sum L_i a_i}{S_i} + \eta_{\text{int}}, \qquad (22)$$

where h_i is the thickness of the floor [m], c_{Li} is the longitudinal wave speed of the plate [m/s], L_i is the perimeter of the plate [m], α_i is the average sound absorption coefficient of the floor, S_i is the area of the floor [m^2], and η_{int} is the internal loss coefficient of the plate.

3.2. Coupling loss factor

There are 4 kinds of couplings between the subsystems of the SEA model. The equations for calculating the coupling loss factors are given below (CRAIK, SMITH, 2000).

The coupling loss factor from plate i to room j is

$$\eta_{ij} = \frac{\rho_0 c_0 \sigma_i}{2\pi f \rho_{si}}; \qquad (23)$$

the coupling loss factor from room i to plate j is

$$\eta_{ij} = \frac{\rho_0 c_0^2 S_j f_{cj} \sigma_j}{8\pi V_i \rho_{sj} f^3}; \qquad (24)$$

the coupling loss factor from cavity i to plate j is

$$\eta_{ij} = \frac{\rho_0 c_0 f_{cj} \sigma_j}{4\pi \rho_{sj} f^2}; \qquad (25)$$

where σ is the radiation efficiency of a floor plate, the ratio of power radiated by a floor plate to that radiated by a piston. The measurement of the radiation efficiencies can be conducted by a standard that has been proposed as Part 5 of the ISO 10848 series (ISO 10848, 2006).

If the floor plate is installed in a frame between two upper and lower reverberation rooms then the radiation efficiency can be determined from the sound power level in the receiving room L_w as determined according to ISO 3741 (ISO 3741, 2010) and the surface velocity of the plate:

$$\sigma = \frac{P_{\text{ref}} 10^{\frac{L_w}{10}}}{S \rho_0 c_0 \overline{\langle v^2 \rangle}}, \qquad (26)$$

where $P_{\text{ref}} = 10^{-12}$ W, S is the surface area of the plate, $\rho_0 c_0$ is the characteristic impedance of air, $\overline{\langle v^2 \rangle}$ is the average mean square surface velocity of the plate.

If the floor plate is installed in a frame in the wall of a semi-anechoic or anechoic chamber and the radiated sound intensity from the side of the plate facing the semi-anechoic room is measured according to

ISO 15186 (ISO 15186, 2000), then the radiation efficiency can be given:

$$\sigma = \frac{I}{\rho_0 c_0 \overline{\langle v^2 \rangle}}, \qquad (27)$$

where I is the measured sound intensity.

The coupling loss factor from cavity i to room j (non-resonant) is

$$\eta_{ij} = \frac{\tau_{ij}}{4\pi}. \qquad (28)$$

The coupling loss factor from floor covering i to floor plate j is

$$\eta_{ij} = \frac{2L\tau_{ij}}{\pi k_i S_j}. \qquad (29)$$

In this paper τ_{ij} is τ_{14}, where L is the boundary length [m], S_j is the area [m^2] of the floor plate, and k_i is the bending wavenumber in floor covering 1.

4. Prediction results and path analysis

The impact sound pressure levels underneath the floating floor with different floor covering, resilient layer, and concrete floor plate are predicted by using the above method, and the sound transmission characteristics and influencing factors on sound insulation are analysed below.

4.1. Comparison between the predicted and measured impact sound pressure levels

The study was carried out on a 22 mm thick composite wood floor covering (the longitudinal wave speed is 3400 m/s, the density is 542 kg/m^3), the section size of the wood stud (the density is 525 kg/m^3) is 45×45 mm, the thickness of the resilient layer (the stiffness is 12 000 kN/m^2) is 12 mm, and the thickness of the reinforced concrete plate (the longitudinal wave speed is 2770 m/s, the density is 2300 kg/m^3) is 140 mm. The density can be found reasonably accurately from published data but obtaining a value for longitudinal wave speed is more difficult. The measurement of longitudinal wave speed can be made in any part of the structure. The setup of the experiment is shown in Fig. 7.
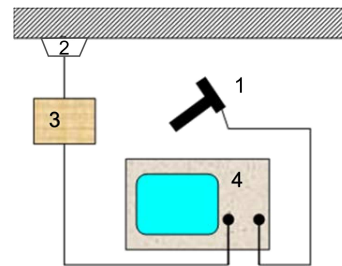

Fig. 7. Measurement of longitudinal wave speed: 1 – plastic hammer with an accelerometer, 2 – accelerometer, 3 – accelerometer charger, 4 – oscilloscope.

The accelerometers are calibrated, and the oscilloscope is adjusted to determine the time base. A plastic hammer with an accelerometer is adopted as a source for hitting the floor plate and generating a pulse. Then, the longitudinal waves are excited in the plate by striking the structure in the direction of sound transmission. The accelerometers detect the pulse and display it on the oscilloscope screen.

At this moment, according to the phase difference of the in-phase sites of the two pulse waves on the oscilloscope, the time difference Δt is converted from the time base, and the distance L between the exciting point and receiving point. The longitudinal wave speed can be calculated:

$$c_L = \frac{L}{\Delta t}. \tag{30}$$

According to the building code on sound insulation measurement of the floor GBT 19889.7-2005 (in China), the standardized impact sound pressure level in the receiving room underneath a floating floor is measured by using the standard tapping machine to excite the floor as the impact sound source. When the tapping machine strikes the floor cover layer, the impact sound transmission across each component of the floating floor structure occurs, and finally the impact sound energy is radiated into the downstairs receiving chamber. Then the impact sound pressure level which radiates from the ceiling can be read by the sound analyser. Finally, the standardised impact sound pressure level L_p can be calculated by the impact sound pressure level and reverberation time in the receiving chamber. The predicted and measured (Chen, 2013) standardised impact sound pressure levels downstairs are shown in Fig. 8.
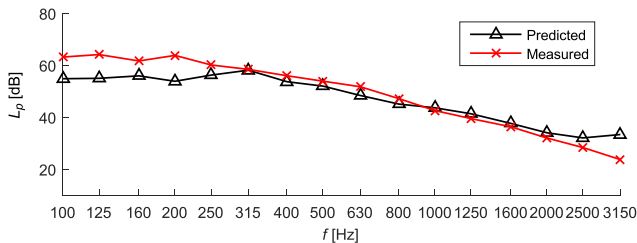

Fig. 8. Measured and predicted standardised impact sound pressure level in the receiving room beneath a floating floor.

The "statistical" in statistical energy analysis means: the statistical properties of these subsystem modes. If statistical averaging is to be meaningful, then there must be several modes. There should be at least 6 modes per band for a floor plate (Craik, 1996; 2000). In this case, the mode density of the floating floor is 0.0728, and the modes per band measure is 4.2 at 250 Hz, therefore, the theoretical prediction underestimates the measured results at the frequencies below 250 Hz due to a low mode density.

There is a favourable agreement between the predicted and measured results in the range of 250–2500 Hz. At 3150 Hz, the prediction approach is a bending wave model, the influence of the longitudinal and transverse waves cannot be ignored at higher frequencies. Meanwhile, the coincidence effects of wood floor covering also result in the discrepancy between measurement and prediction, so the predicted value is higher than the measured value because the model prediction is precise at higher frequency. Thus, there exists a good agreement between the predicted and measured standardised impact sound pressure levels in the downstairs room. The comparison between prediction and measurement shows that the SEA model is an appropriate approach to predict the impact sound insulation of a floating floor.

4.2. Sound transmission path analysis

The dominant path is determined by comparing the sound transmission contributions of the stud path and the cavity path. Three groups of resilient layer materials are cork, closed cell foam and foam laminated fabric, and their properties are listed in Table 1.

Table 1. Configurations of the floating floor with different resilient layers (Stewart, Craik, 2000).

Group	Resilient layer	Stiffness [kN/m^2]	Thickness of concrete floor plate [mm]	Thickness of floor covering [mm]
1	12 mm cork	12000	140	22
2	12 mm closed cell foam	2800	140	22
3	12 mm foam laminated fabric	260	140	22

The stiffness in Table 1 is defined as the ratio of dynamic displacement to dynamic load, and is a significant parameter which has an evident effect on impact sound insulation prediction. Its values, which are provided by standard EN 29052-1 (1993), can be used to determine the acoustical properties of floating floors in a residential building.

Resilient layer stiffness per unit area is evaluated on the basis of the resonance frequency f_{res} measurement of the loading mass resilient layer, as presented in standard EN 29052-1(1993). After measuring the resonance frequency of a resilient layer, the stiffness per unit area of the layer is determined.

The calculated results of the impact sound pressure levels of the cavity path and the stud path are shown in Fig. 9.

The resilient materials used in Figs 9a and 9b are cork and closed cell foam material, and the stud path is always the dominant sound transmission path in the whole frequency range (100–3150 Hz). Due to the coincidence effect, the sound transmission of the cavity
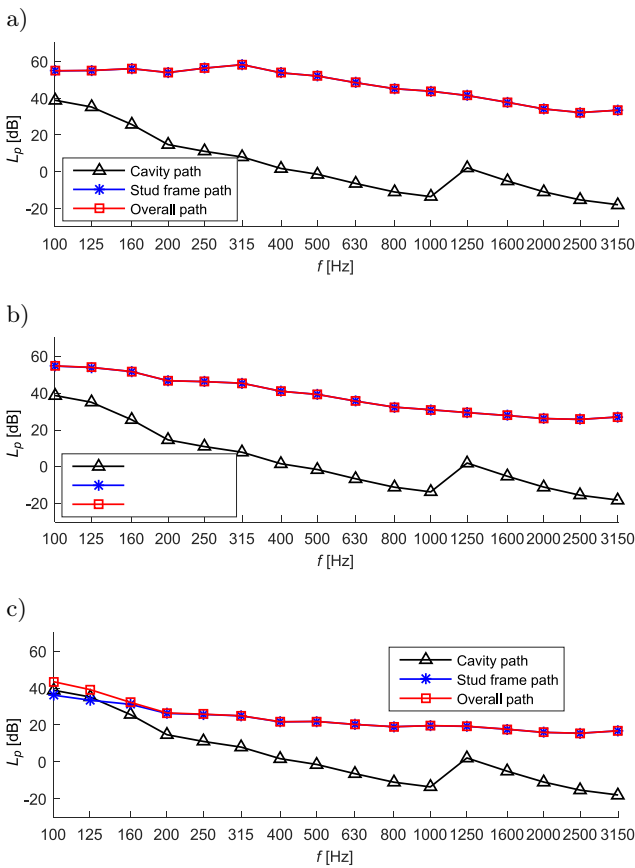
a)

b)

c)

Fig. 9. Impact sound level along different paths in the floating floors with the resilient layers: a) cork, b) closed cell foam, c) foam laminated fabric.

path increases sharply from 1000 to 1250 Hz, but this has almost no effect on the whole sound transmission. The resilient layer material used in Fig. 9c is foam laminated fabric with the lowest stiffness. Below 160 Hz, the cavity path exhibits the dominant transmission path, while above 160 Hz, the stud path becomes the dominant one. It is shown that when the stiffness of the resilient layer is low, the cavity path will tend to be the dominant path at low frequencies. The acoustic energy transmission through the stud path can be effectively prevented by using a resilient material with a low stiffness, and the acoustic bridge effect is obviously weakened. It is indicated that impact sound transmission across the studs is the most important path when there is a resilient layer with high stiffness but that this is less significant for any resilient layer with a low stiffness.

5. Influencing factors of impact sound insulation

5.1. Floor covering

The floor covering (such as chipboard) is fixed to the studs at discrete spaces, and its influence on the impact sound insulation of the floor structure is usually measured in the standard laboratory required by the standard EN ISO 140-8. Because of the limited number of such laboratories and the high cost of their construction, PEREIRA et al. (2014) used the method of scale model to test the influence of several floor coverings on the impact sound insulation of floating floors. They found that the measurement of scale model method is close to the results obtained according to the standard EN ISO140-8 measurement, but there was a lack of a theoretical prediction model. Based on the theoretical prediction model developed in this paper, the effects of 4 kinds of common wood floor covering with different thicknesses (as shown in Table 2) on the impact sound insulation of the floor are studied. The thickness of the flooring varies from 18 mm to 30 mm, and other structural parameters are shown in Table 1. The impact sound pressure level curves of different material and thickness are shown in Figs 10a and 10b, respectively.

Table 2. The floating floor with 4 different kinds of timber floor covering.

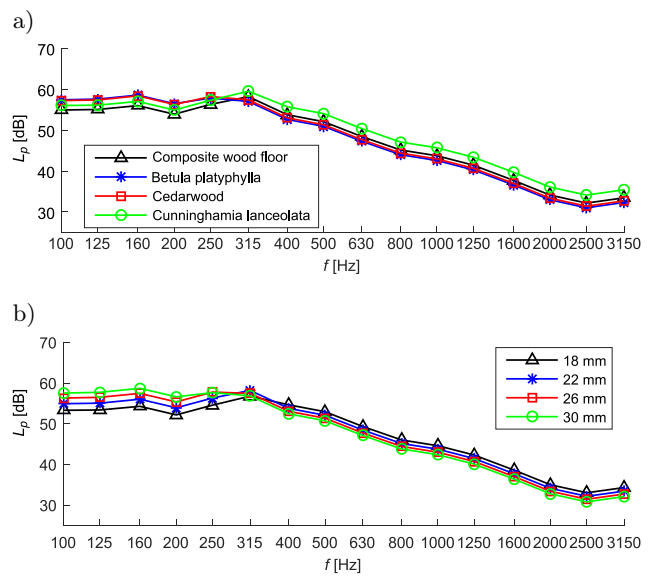| Floor covering	Density $[\text{kg/m}^3]$	Elastic modulus $[\text{N/m}^2]$
Composite wood floor	542	$4 \cdot 10^9$
Betula platyphylla	706.1	$1 \cdot 10^{10}$
Cedarwood	646.6	$1 \cdot 10^{10}$
Cunninghamia lanceolata	345.5	$1 \cdot 10^{10}$

a)

b)

Fig. 10. Standardised impact sound pressure levels for floor coverings with different: a) materials, b) thickness.

At low frequencies, the composite wood floor has a good sound insulation effect below 315 Hz, and when the frequency is above 250 Hz, the impact sound pressure level of the floor with cunninghamia lanceolata covering is higher than that of the other three kinds of floors, which indicates that the impact sound insu-

lation with low density wood floor covering is poor in the middle and high frequency range; and at the same frequency range, the impact sound insulation of betula platyphylla, cypress, and cunninghamia lanceolata floor coverings has no obvious difference. In the whole frequency range, the floating floor with a composite wood floor has the best impact sound insulation. It is shown that the floor covering with low elastic modulus is beneficial for the isolation of impact sound.

Taking composite wood floor as an example, the influence of floor covering thickness on sound insulation is investigated. As seen from Fig. 10b, in most frequency ranges (315–3150 Hz), the thick floor covering exhibits high sound insulation, and at the low frequency range (100–315 Hz), the thin plate is beneficial for the sound insulation.

5.2. Influence of resilient layer

Figure 11a shows the prediction results of the impact sound pressure level of floating floors with different stiffness coefficients K. It can be seen from Fig. 11a that the resilient layer plays a key role in the attenuation of impact sound across a floating floor, and the sound insulation effect of the floor is improved in the whole frequency range (100–3150 Hz). The lower the stiffness coefficient K of the resilient layer, the better the sound insulation effect because it leads to a higher sound transmission loss along the stud path. Due to the insulation of the resilient layer, the sound bridge effect of the stud is weakened. In the higher frequency range, the sound transmission loss increases rapidly because the longitudinal wave cannot be ignored. It can be seen that the resilient layer has a significant improvement on sound insulation at
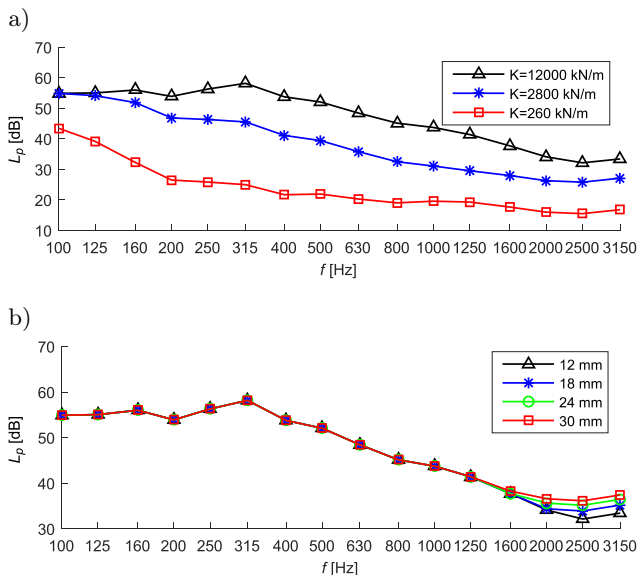
medium and high frequency. Song *et al.* (2000) employed a scale model to evaluate prediction methods of predicting impact sound insulation and also found that the impact sound reduction level increases as the stiffness of resilient layer decreases. Figure 11b shows that the influence of the thickness of the resilient layer on the sound insulation of the floor is reflected in the high frequency range (above 1600 Hz). With the increase of the thickness, sound insulation at high frequencies degrades slightly. Therefore, the isolation effect of the resilient layer depends on its stiffness coefficient, and the thickness almost has no influence on impact sound transmission below 1600 Hz.

5.3. Influence of the thickness of the concrete floor plate

The structural floor plate is generally a reinforced concrete slab, and there is almost no choice of materials, so it is considered that the thickness of the reinforced concrete floor varies from 100 mm to 160 mm. As shown in Fig. 12, the thicker the floor is, the better it is for impact sound insulation, but the improvement is marginal. However, the thickness of the floor plate cannot be too high: 120 mm or 140 mm is suitable.
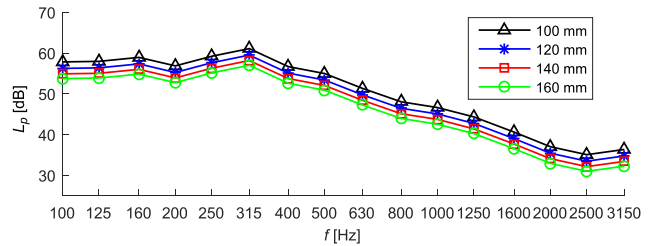

Fig. 12. Influence of concrete floor plate thickness on impact sound insulation.

6. Discussion

In this paper, a theoretical model for predicting the impact sound transmission across a floating floor is developed to include the influence of the floor covering, resilient layer, and the floor plate:

(1) The influence of the floor on the impact sound insulation is also affected by the material properties of the floor covering, but the influence of its thickness is relatively unimportant.

(2) In the aspect of the influence of the resilient layer on the floor impact sound insulation, the stiffness coefficient of the resilient layer has the most significant effect on sound insulation, and the structure borne sound reduction through the stud path can be greatly improved by selecting materials with a low stiffness coefficient. Therefore, the isolation performance of the floating floor in impact sound and vibration mainly depends on the dynamic

Fig. 11. Prediction value of impact sound pressure level of floating floor with different: a) stiffness coefficient, b) layer thickness.

characteristics of the resilient materials. Additionally, the lower the stiffness coefficient of the resilient layer material, the wider the frequency range in which the cavity path becomes the dominant sound transmission path.

(3) The impact sound insulation increases with the thickness of the floor plate gradually, which can generally be set to 120 mm or 140 mm.

According to the discussion above, different scenarios can be implemented to achieve the optimum solution; i.e., the optimised floating floor structure can be determined as follows: lower elastic modulus, thicker floor covering, and resilient layer with a low stiffness coefficient.

7. Conclusions

Floating floors in a residential building are adopted to attenuate the impact noise, such as structure borne sounds generated from walking or moving furniture on the upper floor. A theoretical model theory has been presented to explore the effect of impact sound transmission across a floating floor. The main goal of this study was to determine the standardised sound pressure level in the receiving room underneath the float-

ing floor. Based on the analysis of the sound transmission path, the impact sound pressure level prediction model of the floating floor was established by using SEA. Although the model has a slight difference in the low frequency prediction, in other frequency ranges, the predicted value of standardised impact sound pressure level agrees well with the measured results. Moreover, the path analysis of SEA provides a clear description of the sound transmission path across a floating floor, i.e. the impact sound is transmitted to the downstairs room through the stud path and the cavity path. The prediction results show that in most cases, the stud path is the most significant sound transmission path. If there is a resilient layer, the sound transmission of the path will be effectively suppressed, thus improving the impact sound insulation greatly. Then, as the influencing factors of sound insulation of a floating floor are analysed, it reveals that the floor structure with a low stiffness interlayer and a low elastic modulus, thicker floor covering might be beneficial for impact sound insulation.

Acknowledgments

Appendix

Table 3. Loss factors and coupling loss factors used in Eqs (3)–(20).

f [Hz]	η_{12}	η_{25}	η_1	η_2	η_4	η_{24}	η_{45}
100	$4.87 \cdot 10^{-4}$	$1.52 \cdot 10^{-4}$	$4.38 \cdot 10^{-2}$	$7.86 \cdot 10^{-3}$	$8.74 \cdot 10^{-2}$	$2.67 \cdot 10^{-4}$	$3.87 \cdot 10^{-4}$
125	$4.36 \cdot 10^{-4}$	$7.79 \cdot 10^{-5}$	$4.07 \cdot 10^{-2}$	$6.29 \cdot 10^{-3}$	$7.89 \cdot 10^{-2}$	$1.91 \cdot 10^{-4}$	$3.46 \cdot 10^{-4}$
160	$3.85 \cdot 10^{-4}$	$3.72 \cdot 10^{-5}$	$3.78 \cdot 10^{-2}$	$4.91 \cdot 10^{-3}$	$7.06 \cdot 10^{-2}$	$1.44 \cdot 10^{-3}$	$3.35 \cdot 10^{-3}$
200	$3.45 \cdot 10^{-4}$	$1.90 \cdot 10^{-5}$	$3.54 \cdot 10^{-2}$	$3.93 \cdot 10^{-3}$	$6.39 \cdot 10^{-2}$	$6.17 \cdot 10^{-4}$	$1.79 \cdot 10^{-3}$
250	$3.08 \cdot 10^{-4}$	$9.74 \cdot 10^{-6}$	$3.32 \cdot 10^{-2}$	$3.14 \cdot 10^{-3}$	$5.79 \cdot 10^{-2}$	$3.29 \cdot 10^{-4}$	$1.19 \cdot 10^{-3}$
315	$2.75 \cdot 10^{-4}$	$4.87 \cdot 10^{-6}$	$3.12 \cdot 10^{-2}$	$2.49 \cdot 10^{-3}$	$5.23 \cdot 10^{-2}$	$1.85 \cdot 10^{-4}$	$8.46 \cdot 10^{-4}$
400	$2.44 \cdot 10^{-4}$	$2.38 \cdot 10^{-6}$	$2.94 \cdot 10^{-2}$	$1.96 \cdot 10^{-3}$	$4.72 \cdot 10^{-2}$	$1.06 \cdot 10^{-4}$	$6.18 \cdot 10^{-4}$
500	$2.18 \cdot 10^{-4}$	$1.22 \cdot 10^{-6}$	$2.79 \cdot 10^{-2}$	$1.57 \cdot 10^{-3}$	$4.30 \cdot 10^{-2}$	$6.47 \cdot 10^{-5}$	$4.70 \cdot 10^{-4}$
630	$1.94 \cdot 10^{-4}$	$6.09 \cdot 10^{-7}$	$2.65 \cdot 10^{-2}$	$1.25 \cdot 10^{-3}$	$3.90 \cdot 10^{-2}$	$3.93 \cdot 10^{-5}$	$3.59 \cdot 10^{-4}$
800	$1.72 \cdot 10^{-4}$	$2.97 \cdot 10^{-7}$	$2.52 \cdot 10^{-2}$	$9.82 \cdot 10^{-4}$	$3.54 \cdot 10^{-2}$	$2.37 \cdot 10^{-5}$	$2.75 \cdot 10^{-4}$
1000	$1.54 \cdot 10^{-4}$	$1.52 \cdot 10^{-7}$	$2.41 \cdot 10^{-2}$	$7.86 \cdot 10^{-4}$	$3.24 \cdot 10^{-2}$	$1.48 \cdot 10^{-5}$	$2.15 \cdot 10^{-4}$
1250	$1.12 \cdot 10^{-2}$	$7.79 \cdot 10^{-8}$	$2.31 \cdot 10^{-2}$	$6.29 \cdot 10^{-4}$	$2.97 \cdot 10^{-2}$	$9.34 \cdot 10^{-6}$	$1.70 \cdot 10^{-4}$
1600	$5.83 \cdot 10^{-3}$	$3.72 \cdot 10^{-8}$	$2.22 \cdot 10^{-2}$	$4.91 \cdot 10^{-4}$	$2.71 \cdot 10^{-2}$	$5.63 \cdot 10^{-6}$	$1.31 \cdot 10^{-4}$
2000	$3.95 \cdot 10^{-3}$	$1.90 \cdot 10^{-8}$	$2.14 \cdot 10^{-2}$	$3.93 \cdot 10^{-4}$	$2.50 \cdot 10^{-2}$	$3.57 \cdot 10^{-6}$	$1.04 \cdot 10^{-4}$
2500	$2.85 \cdot 10^{-3}$	$9.74 \cdot 10^{-9}$	$2.08 \cdot 10^{-2}$	$3.14 \cdot 10^{-4}$	$2.31 \cdot 10^{-2}$	$2.27 \cdot 10^{-6}$	$8.23 \cdot 10^{-5}$
3150	$2.11 \cdot 10^{-3}$	$4.87 \cdot 10^{-9}$	$2.01 \cdot 10^{-2}$	$2.49 \cdot 10^{-4}$	$2.13 \cdot 10^{-2}$	$1.42 \cdot 10^{-6}$	$6.49 \cdot 10^{-5}$

Table 4. Parameters used in equation Eqs (3)–(20).

E_1 [N/m^2]	E_4 [N/m^2]	K [kN/m^2]	f_{c4} [Hz]	c_L [m/s]
$4.0 \cdot 10^9$	$2.5 \cdot 10^{10}$	$1.2 \cdot 10^{10}$	136.3	178.9

References

1. CHEN X. (2013), *Laboratory measurements of the reduction of transmitted impact noise by wooden floors*, Master's Thesis, South China University of Technology, Guangzhou, China.

2. CHO T. (2013), Experimental and numerical analysis of floating floor resonance and its effect on impact sound transmission, *Journal of Sound and Vibration*, **332**(25): 6552–6561, doi: 10.1016/j.jsv.2013.08.011.

3. CRAIK R.J.M. (1996), *Sound Transmission Through Building Using Statistical Energy Analysis*, Gower Publishing Limited, Aldershot, England.

4. CRAIK R.J.M. (2000), *Advanced Building Acoustics*, p. 7, Heriot-Watt University, Edinburgh.

5. CRAIK R.J.M., SMITH R.S. (2000), Sound transmission through lightweight parallel plates. Part II: Structure-borne sound, *Applied Acoustics*, **61**(2): 247–269, doi: 10.1016/S0003-682X(99)00071-7.

6. EN 29052-1/1993(1993): *Acoustics – determination of dynamic stiffness – materials used under floating floor in dwellings.*

7. HUI C.K., NG C.F. (2007), New floating floor design with optimum isolator location, *Journal of Sound and Vibration*, **303**(1–2): 221–238, doi: 10.1016/j.jsv.2007.01.011.

8. ISO 10848-1:2006 (2006), *Acoustics – Laboratory measurement of the flanking transmission of airborne and impact sound between adjoining rooms – Part 1: Frame document*, Geneva, Switzerland: International Standards Organization.

9. ISO 15186-1:2000 (2000), *Acoustics – Measurement of sound insulation in buildings and of building elements using sound intensity – Part 1: Laboratory measurements*, Geneva, Switzerland: International Standards Organization.

10. ISO 3741:2010 (2010), *Acoustics – Determination of the sound power levels and sound energy levels of noise sources using sound pressure – Precision methods for reverberation test rooms*, Geneva, Switzerland: International Standards Organization.

11. KIM K., JEONG G., YANG K., SOHN J. (2009), Correlation between dynamic stiffness of resilient materials and heavyweight impact sound reduction level, *Building and Environment*, **44**(8): 1589–1600, doi: 10.1016/j.buildenv.2008.10.005.

12. KIM T.M., KIM J.T., KIM J.S. (2018), Effect of structural vibration and room acoustic modes on low frequency impact noise in apartment house with floating floor, *Applied Acoustics*, **142**, 59–69, doi: 10.1016/j.apacoust.2018.07.034.

13. LEE E.G. (2009), Noise control regulation of the United Kingdom of Great Britain, *Environ. Law Review*, **31**(3): 187.

14. LI Q., YANG X., ZANG X. (2017), Design of sound-proof residential construction based on DB13(J)/T113-2015 evaluation standards for green buildings, *Building Science*, **33**(12): 172–176.

15. LJUNGGREN F., AGREN A. (2013), Elastic layer to reduce sound transmission in lightweight buildings, *Building Acoustics*, **20**(1): 25–42, doi: 10.1260/1351-010X.20.1.25.

16. LUO C., HU X. (2012), Investigation and analysis of the floor impact sound insulation measures, *Building and Culture*, **7**: 88–89.

17. NEVES E SOUSA A., GIBBS B.M. (2011), Low frequency impact sound transmission in dwellings through homogeneous concrete floors and floating floors, *Applied Acoustics*, **72**(4): 177–189, doi: 10.1016/j.apacoust.2010.11.006.

18. OLSSON J., LINDERHOLT A. (2019), Force to sound pressure frequency response measurements using a modified tapping machine on timber floor structures, *Engineering Structures*, **196**: 109343, doi: 10.1016/j.engstruct.2019.

19. PARK H.S., OH B.K., KIM Y., CHO T. (2015), Low frequency impact sound transmission of floating floor: case study of mortar bed on concrete slab with continuous interlayer, *Building and Environment*, **94**(Part 2): 793–801, doi: 10.1016/j.buildenv.2015.06.005.

20. PARK K.H. (2015), Criminal study on the noise: focused on the floor impact noise dispute, *Inha Law Review*, **18**(3): 297–328.

21. PEREIRA A., GODINHO L., MATEUS D., RAMIS J., BRANCO F.G. (2014), Assessment of a simplified experimental procedure to evaluate impact sound reduction of floor coverings, *Applied Acoustics*, **79**: 92–103, doi: 10.1016/j.apacoust.2013.12.014.

22. SCHIAVI A. (2018), Improvement of impact sound insulation: A constitutive model for floating floors, *Applied Acoustics*, **129**: 64–71, doi: 10.1016/j.apacoust.2017.07.013.

23. SCHIAVI A., PRATO A., BELLI A.P. (2015), The "dust spring effect" on the impact sound reduction measurement accuracy of floor coverings in laboratory, *Applied Acoustics*, **97**: 115–120, doi: 10.1016/j.apacoust.2015.04.011.

24. SONG M.J., JANG G.S., KIM S.W. (2000), An experimental study on the prediction method of light weight floor impact sound insulation performance of apartment floor structures through mini-laboratory tests, *Transactions of the KSNVE 2000*, **10**: 82–98.

25. STEWART M.A., CRAIK R.J.M. (2000), Impact sound transmission through a floating floor on a concrete slab, *Applied Acoustics*, **59**(4): 353–372, doi: 10.1016/S0003-682X(99)00030-4.

26. TOMLINSON D., CRAIK R.J.M., WILSON R. (2004), Acoustic radiation from a plate into a porous medium,

Journal of Sound and Vibration, **237**(1–2): 33–49, doi: 10.1016/j.jsv.2003.04.003.

27. Vigran E. (2008), *Building Acoustics*, pp. 232–262, Taylor & Francis Group, London.

28. Yeon J.O., Kim K.W., Yang K.S. (2017), A correlation between a single number quantity and noise level of real impact sources for floor impact sound,

Applied Acoustics, **125**: 20–33, doi: 10.1016/j.apacoust.2017.03.019.

29. Yoo S.Y., Jeon J.Y. (2014), Investigation of the effects of different types of interlayers on floor impact sound insulation in box-frame reinforced concrete structures, *Building and Environment*, **76**: 105–112, doi: 10.1016/j.buildenv.2014.03.008.